STRUCTURAL BIOLOGY COMMUNICATIONS

ISSN 2053-230X

Binding of Gd^{3+} to the neuronal signalling protein calexcitin identifies an exchangeable Ca^{2+}-binding site

Lucas Chataigner,[a] Jingxu Guo,[a] Peter T. Erskine,[a,b] Alun R. Coker,[a] Steve P. Wood,[a] Zoltan Gombos[c]‡ and Jonathan B. Cooper[a,b]*

[a]Division of Medicine, UCL, Gower Street, London WC1E 6BT, England, [b]Department of Biological Sciences, Birkbeck, University of London, Malet Street, Bloomsbury, London WC1E 7HX, England, and [c]Department of Biological Sciences, University of Alberta, Edmonton, Alberta T6G 2E9, Canada. *Correspondence e-mail: jon.cooper@ucl.ac.uk

Received 21 December 2015
Accepted 29 February 2016

Edited by R. A. Pauptit, Macclesfield, England

‡ Current address: Marketed Health Products Directorate, Health Products and Food Branch, Health Canada, Address Locator 0701L, Ottawa, Ontario K1A 0K9, Canada.

Keywords: neuronal calcium signalling; EF-hand; protein structure; heavy-atom complex; co-crystallization.

PDB reference: calexcitin–Gd^{3+} complex, 5f6t

Supporting information: this article has supporting information at journals.iucr.org/f

Calexcitin was first identified in the marine snail *Hermissenda crassicornis* as a neuronal-specific protein that becomes upregulated and phosphorylated in associative learning. Calexcitin possesses four EF-hand motifs, but only the first three (EF-1 to EF-3) are involved in binding metal ions. Past work has indicated that under physiological conditions EF-1 and EF-2 bind Mg^{2+} and Ca^{2+}, while EF-3 is likely to bind only Ca^{2+}. The fourth EF-hand is nonfunctional owing to a lack of key metal-binding residues. The aim of this study was to use a crystallographic approach to determine which of the three metal-binding sites of calexcitin is most readily replaced by exogenous metal ions, potentially shedding light on which of the EF-hands play a 'sensory' role in neuronal calcium signalling. By co-crystallizing recombinant calexcitin with equimolar Gd^{3+} in the presence of trace Ca^{2+}, EF-1 was shown to become fully occupied by Gd^{3+} ions, while the other two sites remain fully occupied by Ca^{2+}. The structure of the Gd^{3+}–calexcitin complex has been refined to an R factor of 21.5% and an R_{free} of 30.4% at 2.2 Å resolution. These findings suggest that EF-1 of calexcitin is the Ca^{2+}-binding site with the lowest selectivity for Ca^{2+}, and the implications of this finding for calcium sensing in neuronal signalling pathways are discussed.

1. Introduction

A central endeavour in the field of neuroscience is to understand the complex information processing performed by biological neural networks that underlies animal behaviour. Paramount to this pursuit is the investigation of the processes of learning and memory, as well as the biophysical and molecular mechanisms that make such processes possible (Giese *et al.*, 2001). Owing to the complexity of vertebrate nervous systems, initial insights into the molecular basis of memory have been obtained from more amenable experimental invertebrate models with far simpler neural networks, containing many orders of magnitude fewer neurons (Alkon, 1983).

In much of the seminal work of Alkon and coworkers, memory-specific biochemical changes were investigated using a classical Pavlovian conditioning paradigm in *Hermissenda crassicornis*. In this nudibranch mollusc, pairing of light and rotation creates an association between the usually attractive stimulus of light and foot retraction, which is usually an aversive response to movement. Studies of changes in neuronal physiology and molecular composition of photoreceptor cells that correlated specifically with the learned behaviour were undertaken (Nelson & Alkon, 1988, 1990, 1997; Alkon, 1979; Alkon *et al.*, 1990; Kawai *et al.*, 2002). This work demonstrated the upregulation and phosphorylation of a

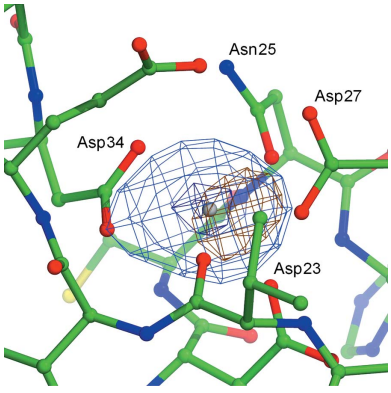

neuron-specific ~20 kDa protein (Neary *et al.*, 1981), which was subsequently termed calexcitin. This protein was found to have GTPase activity and could reproduce the electrophysiological effects of conditioning when injected into photoreceptor cells (Nelson *et al.*, 1990). Furthermore, it was found that phosphorylation of calexcitin, which is mediated by protein kinase C, caused its translocation from cytosolic to membrane fractions (Nelson & Alkon, 1995).

Cloning and sequencing of a squid homologue of calexcitin from the optic lobe of *Loligo pealei* (Nelson *et al.*, 1996) showed a number of interesting features such as the presence of three functional EF-hand binding motifs which form Ca^{2+}- and Mg^{2+}-binding sites (Gombos *et al.*, 2001). Electrophysiological studies using recombinant squid calexcitin and human fibroblast inside-out patches also showed that the protein is capable of directly regulating K^+-channel mean open time and probability in the presence of Ca^{2+} (Nelson *et al.*, 1996). Furthermore, investigation using sensory and chemical blocks during learning in *Hermissenda* established calexcitin as being necessary to establish and consolidate long-term memory (Kuzirian *et al.*, 2001, 2003; Borley *et al.*, 2002; Child *et al.*, 2003; Epstein *et al.*, 2003). Additional experimental evidence has also implicated calexcitin in several mechanisms that could enable it to functionally alter neuronal physiology. Presynaptically, calexcitin is thought to be a key constituent of terminal nerve endings (Eyman *et al.*, 2003) and to regulate retrograde axonal transport (Moshiach *et al.*, 1993). Furthermore, postsynaptically it may alter dendritic morphology upon phosphorylation (Lederhendler *et al.*, 1990) and can transform synaptic outputs from inhibitory to excitatory potentials (Sun *et al.*, 1999). Noteworthy evidence has furthermore suggested that its postsynaptic effects could result from the modulation of intracellular Ca^{2+} levels by direct interaction with the ryanodine receptor, facilitating Ca^{2+} release from intracellular stores (Nelson *et al.*, 1999). Although calexcitin shows the highest homology to the sarcoplasmic calcium-binding protein (SCP) family, past work identified protein features consistent with a calcium-sensor function.

X-ray and NMR structural studies ultimately demonstrated that calexcitin is primarily an α-helical protein organized into two separate domains, each with two EF-hand motifs, although the last one is nonfunctional (Erskine *et al.*, 2006; Gombos *et al.*, 2006). The two domains appear to adopt a closed conformation with a pronounced hydrophobic core which is similar to that found in calmodulin, suggesting that domain movements allow calexcitin to interact with binding-partner proteins (Erskine *et al.*, 2006; Gombos *et al.*, 2003). The most recent data from NMR and molecular-simulation studies suggested that the domains have sufficient flexibility in solution to allow opening of the inter-domain hydrophobic cleft (Erskine *et al.*, 2015).

Titration studies have indicated that calexcitin has different affinities for Ca^{2+} ions depending on the Mg^{2+} concentration (Gombos *et al.*, 2003). In the absence of Mg^{2+} the apparent K_d for Ca^{2+} is 0.77 μM (range 0.37–3.3 μM), which changes to 2.58 μM (range 1.5–4.8 μM) in the presence of 2 mM Mg^{2+}. In quiescent neurons the Ca^{2+} concentation is in the 10–100 nM range and the presence of Mg^{2+} means that even the high-affinity site(s) will probably not be occupied by Ca^{2+}. During cellular activation, the intracellular level of Ca^{2+} increases to the micromolar range and can be further elevated in particular cellular compartments. Thus, it is likely that all three sites will be occupied by Ca^{2+} during neuronal activation.

There is uncertainty as to which of the metal-binding sites of calexcitin has a sensory role in the neuron and also as to how the sites give rise to the different measurable Ca^{2+} affinities (Gombos *et al.*, 2003). Our aim is to define how the metal-binding sites of this protein allow it to act as a calcium sensor in a similar manner to calmodulin, which is known to adopt a significantly different structure at high Ca^{2+} concentration. Understanding the structural basis of calcium sensing by EF-hand proteins is an important objective in defining how intracellular signalling pathways operate. To address some of these questions, we have crystallized recombinant calexcitin in calcium-free buffer in the presence of an equimolar concentration of the heavy atom gadolinium and only trace Ca^{2+}. Lanthanide ions such as Gd^{3+} are well known for binding at Ca^{2+}-binding sites in proteins owing to their unique chemical property known as lanthanide contraction. This arises from poorer shielding of valence electrons by the 4f electrons in the lanthanide elements, such that the increase in nuclear charge across this series of the periodic table causes an enhanced reduction in ionic radius. We have co-crystallized calexcitin with equimolar Gd^{3+} in the presence of only trace Ca^{2+} and determined the structure at 2.2 Å resolution, demonstrating that Gd^{3+} binds at EF-1, the first EF-hand in the N-terminal domain of the protein, and suggesting that this is the site with the lowest selectivity for Ca^{2+}.

2. Methods

2.1. Expression and crystallization of the calexcitin–Gd^{3+} complex

His-tagged *L. pealei* calexcitin was expressed in *Escherichia coli* and purified as described previously (Beaven *et al.*, 2005; Erskine *et al.*, 2006), except that protease inhibitors were not used during purification. A 1 ml aliquot of purified calexcitin at a concentration of 4 mg ml^{-1} was dialyzed overnight against a 1 l volume of 50 mM Tris pH 7.5, 100 mM NaCl, 1 mM β-mercaptoethanol that was made without adding any $CaCl_2$, which is normally present in the crystallization buffer at a concentration of 1 mM. After dialysis, the protein at a concentration of 2.6 mg ml^{-1} (60 μM) was mixed with $GdCl_3$ to give an equimolar ratio and was subjected to the Morpheus HT-96 (Gorrec, 2009) and PACT premier HT-96 (Newman *et al.*, 2005) crystal screens using a Mosquito robot (TTP Labtech) to mix 400 nl well solution and 400 nl protein solution. Molecular Dimensions Structure Screens 1 + 2 (Jancarik & Kim, 1991; Wooh *et al.*, 2003) were also used in 24-well plate format by mixing 3 µl well solution and 3 µl protein solution. Crystals suitable for diffraction experiments were obtained from two Structure Screen 1 conditions (0.2 M sodium acetate trihydrate, 0.1 M sodium cacodylate pH 6.5, 30% PEG 8000

and 0.2 *M* sodium acetate trihydrate, 0.1 *M* Tris pH 8.5, 30% PEG 4000). Crystals from the latter condition were cryoprotected by the addition of glycerol to a final concentration of 30%, mounted in 0.2 mm LithoLoops (Molecular Dimensions) on 18 mm CrystalCap pins (Hampton Research) and finally flashed-cooled in a nitrogen-gas cryostream (Oxford Cryosystems) at a temperature of 100 K for storage in liquid nitrogen.

2.2. X-ray data collection and processing

Synchrotron X-ray data for the calexcitin co-crystals were collected on the I04 beamline at the Diamond Light Source facility (DLS), Didcot, England using a Pilatus 6M-F detector. A total of 190 images, each with an oscillation angle of 1° and an exposure time of 3 s, were recorded with a beam size of 20 × 20 µm and a transmission of 33%. The data were processed with *MOSFLM* (Leslie & Powell, 2007) and scaled using *SCALA* (Evans, 2006) in the *CCP*4 program suite (Winn *et al.*, 2011), keeping the Friedel mates separate to allow analysis of anomalous differences. The scaling statistics for alternative point groups and inspection of systematic absences indicated that the space group was either $P4_1$ or $P4_3$, with unit-cell parameters $a = b = 77.0$, $c = 29.3$ Å. Use of the *MATTPROB* server (Kantardjieff & Rupp, 2003) indicated that the crystals contained one molecule per asymmetric unit, with a solvent content of 38%. The structure was determined by molecular replacement with a monomer of the native protein (PDB entry 2ccm; Erskine *et al.*, 2006) as the search model. *Phaser* (McCoy *et al.*, 2007) found a solution in space group $P4_3$, and the resulting maps were interpreted using *Coot* (Emsley & Cowtan, 2004; Emsley *et al.*, 2010) prior to refinement of the model using *REFMAC*5 (Murshudov *et al.*, 1997, 2011) and *PHENIX* (Adams *et al.*, 2010). The latter program was used for the refinement of group TLS parameters, and the metal anomalous scattering factors were refined using the $I(+)$ and $I(-)$ data. The resulting structure and data have been deposited in the Protein Data Bank with identifier 5f6t.

Table 1
X-ray data-processing and refinement statistics for the calexcitin–Gd^{3+} complex.

Values in parentheses are for the outer resolution shell.

Beamline	I04, DLS
Wavelength (Å)	0.9173
Space group	$P4_3$
Unit-cell parameters	
$a = b$ (Å)	77.0
c (Å)	29.3
Solvent content (%)	37.7
No. of monomers per asymmetric unit	1
Matthews coefficient (Å^3 Da^{-1})	2.0
Mosaic spread (°)	0.8
Resolution (Å)	29.3–2.2 (2.3–2.2)
R_{merge}† (%)	13.7 (139.0)
R_{meas}‡ (%)	15.2 (156.4)
$CC_{1/2}$§ (%)	99.6 (34.8)
Completeness (%)	100.0 (100.0)
Average $I/\sigma(I)$	7.5 (1.5)
Multiplicity	6.1 (6.0)
No. of observed reflections	54653
No. of unique reflections	9020
Wilson plot B factor (Å^2)	66.2
R factor (%)	21.5 (39.6)
Free R factor (%)	30.4 (46.8)
R.m.s.d., bond lengths (Å)	0.009
R.m.s.d., bond angles (°)	1.058
No. of $I(+)$ and $I(-)$ in working set	16100
No. of reflections in test set	870
Mean protein B factor (Å^2)	61.5

† $R_{merge} = \sum_{hkl}\sum_i |I_i(hkl) - \langle I(hkl)\rangle| / \sum_{hkl}\sum_i I_i(hkl)$. ‡ $R_{meas} = \sum_{hkl}\{N(hkl)/[N(hkl)-1]\}^{1/2}\sum_i |I_i(hkl) - \langle I(hkl)\rangle| / \sum_{hkl}\sum_i I_i(hkl)$. § Half-set correlation coefficients of Karplus & Diederichs (2012).

3. Results

Data-processing and refinement statistics for the gadolinium complex are shown in Table 1, where it can be seen that the

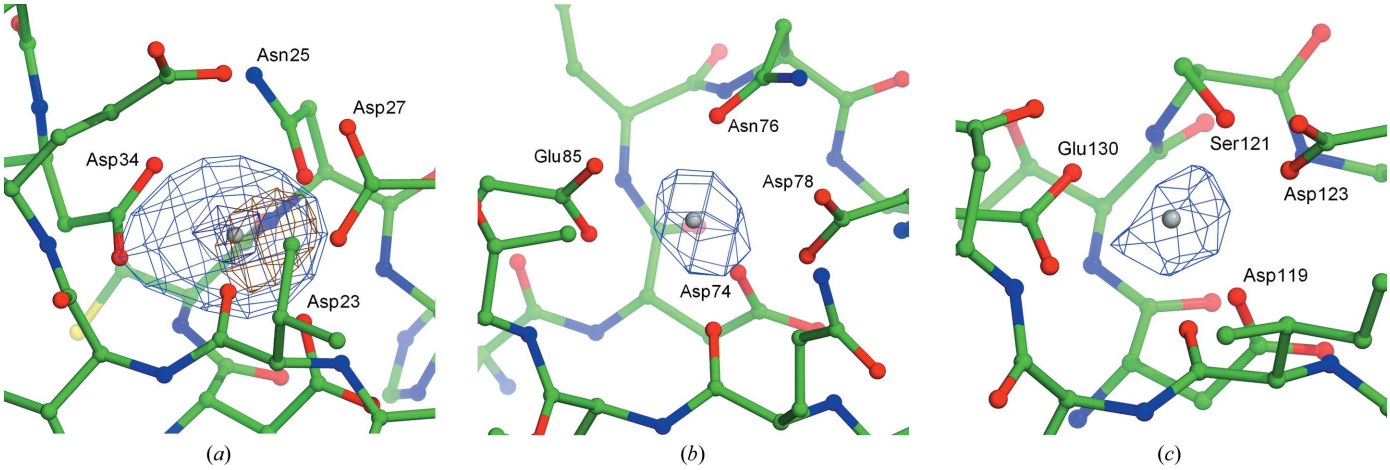

Figure 1
The difference electron density for the three metal-binding sites of calexcitin co-crystallized with equimolar Gd^{3+} in the presence of trace Ca^{2+}. The Ca^{2+}-binding sites formed by EF-hands 1–3 are shown in (*a*), (*b*) and (*c*), respectively, with the final refined position of each metal ion shown by a grey sphere. The OMIT electron density is contoured at 5 r.m.s. (blue) and at 15 r.m.s. (dark blue). A peak in EF-1 exceeding 18 r.m.s. indicated the presence of Gd^{3+}, whereas EF-2 and EF-3 had peaks of around 7 r.m.s., indicating that these retain Ca^{2+}. Accordingly, significant anomalous difference density (contoured at 5 r.m.s. and shown in brown) was only found at EF-1. Each view is oriented such that the bidentate ligand (Asp34, Glu85 and Glu130) is on the left.

R-factor values are slightly worse than would be expected for a structure of this resolution; we attribute this to crystal quality since the diffraction spots displayed some splitting. However, radiation damage did not seem to be significant during data collection.

The electron-density map obtained for the gadolinium co-crystal showed a large peak of positive difference density (18.3 r.m.s.) at EF-1 (Fig. 1). Since all metal ions were omitted from the model at this stage, positive difference density was expected at the remaining two calcium-binding sites, and accordingly peaks of 7.6 r.m.s. and 6.7 r.m.s. were found at EF-2 and EF-3, respectively, suggesting that these are still occupied by Ca^{2+} rather than Gd^{3+}. The binding of Gd^{3+} to EF-1 was corroborated by the calculation of an anomalous difference map in which the highest peak (6.7 r.m.s.) was found to occur at this site, whereas no significant peaks were found at EF-2 or EF-3. In the complex Gd^{3+} is the only significant anomalous scatterer, with a theoretical f'' of 6 e at the wavelength used for data collection (0.92 Å). The final model of the crystal structure contains a Gd^{3+} ion bound at EF-1, with Ca^{2+} ions bound at EF-2 and EF-3 and 30 water molecules. This model was refined using data within a resolution range of 27.4–2.2 Å to an *R* factor of 21.50% and an R_{free} of 30.44%. Structure validation by *MolProbity* (Davis *et al.*, 2007; Chen *et al.*, 2010) showed that 88% of residues were within the most favoured region of the Ramachandran plot and no residues were classed as outliers. The model has a mean isotropic *B*-factor value of 61.10 $Å^2$ for all atoms in the model, which is a rather high value, but this again is probably a reflection of crystal quality. Validation of the metal-binding site geometry with *CheckMyMetal* (Zheng *et al.*, 2014) indicated that the model of the Gd^{3+}-binding site is plausible.

The structure of the Gd^{3+} complex superimposes with the native structure of calexcitin with a C^{α} r.m.s. deviation of 0.66 Å (Fig. 2). This value is slightly higher than might be expected, but is best explained by the different crystal-packing environment of the complex, which is non-isomorphous with the native structure. Accordingly, the regions with the largest deviations are the non-EF-hand loops, which interact with symmetry-related molecules in the two crystal forms and lack the stabilizing influence of a bound metal ion. The metal-binding geometry of the Gd^{3+} site is very similar to that of the native Ca^{2+}-bound protein, emphasizing that Gd^{3+} is a judicious choice to replace Ca^{2+}. The structures of the other metal-binding sites (EF-2 and EF-3) are very similar to those of the native protein, as would be expected since these are most likely to have retained Ca^{2+}. However, the metal-bound water molecules, which are visible in the higher resolution electron density for the native protein, do not appear to be resolved in the map for the Gd^{3+} complex and this is likely to be owing to the higher mean *B* factor of the Gd^{3+} complex as well as the lower crystal and data quality, which are typical of heavy-atom-substituted proteins.

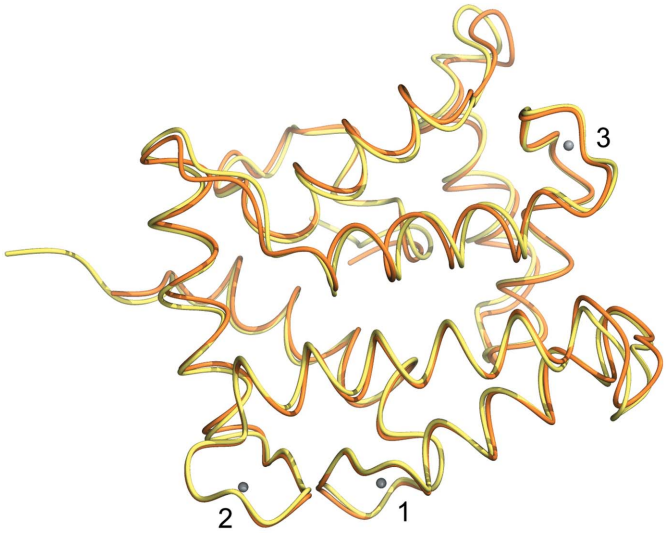

Figure 2
Superposition of the structure of the calexcitin–Gd^{3+} complex with the native protein. The folds of the Gd^{3+} complex and the native protein are coloured gold and cream, respectively, and the metal-binding sites, numbered 1–3, are shown as grey spheres.

4. Discussion

We have determined the structure of the neuronal signalling protein calexcitin crystallized in the presence of equimolar Gd^{3+} and only trace levels of Ca^{2+}. Since Gd^{3+} was found to bind exclusively at EF-1, this site may be the most prone to binding exogenous metal ions when the protein is in a low Ca^{2+} concentration. The conditions of our experiment were such that the protein was partially demetallated by dialysis prior to the addition of Gd^{3+}. Our finding that Gd^{3+} binds exclusively to EF-1 suggests that this is the first site to lose its Ca^{2+} ion as the Ca^{2+} concentration decreases. Indeed, earlier studies suggested that the N-terminal domain has mixed Ca^{2+}/Mg^{2+}-binding sites and that the C-terminal site has a higher specific affinity for Ca^{2+} (Gombos *et al.*, 2003). Thus, we propose that EF-2 and EF-3 retained a bound Ca^{2+} ion following the dialysis step. It is interesting that the second site has a number of acidic residues nearby such that a Ca^{2+} ion attempting to dissociate might be rapidly pulled back by electrostatic forces. The unique structural nature of EF-3, owing to the lack of a functional partner EF-hand in the C-terminal domain and its proximity to the unusual C-terminal 3_{10}-helix which is implicated in GTPase activity, make it difficult to speculate on its relative affinity for calcium ions, but our results suggest that it is also a high-affinity Ca^{2+}-binding site. Our suggestion that EF-1 is the first to lose its bound Ca^{2+} as the buffer Ca^{2+} concentration decreases is consistent with the occurrence of an aspartate residue (Asp34) as the bidentate metal ligand (Fig. 1). In contrast, EF-2 and EF-3 have glutamate residues at this position (Glu85 and Glu130) and this is associated with high selectivity for Ca^{2+}. Indeed, mutational studies of other EF-hand proteins have shown that the presence of aspartate rather than glutamate as the bidentate metal ligand decreases the selectivity for Ca^{2+} (see, for example, Cox *et al.*, 1979; Da Silva *et al.*, 1995; Cates *et al.*, 1999). In addition, this finding is in agreement with studies on calmodulin, which showed that Mg^{2+} preferentially binds to

EF-1 and EF-4 in the absence of Ca^{2+} and that EF-3 has the lowest affinity for Mg^{2+} (Ohki *et al.*, 1997). It is worth remembering that the fourth EF-hand of calexcitin has lost its ability to bind metal ions, which might be owing to its putative GTPase activity.

Our evidence that EF-1 of calexcitin has the lowest Ca^{2+}-affinity site is significant since it opens an interesting line of enquiry into how metal binding triggers structural transitions that enable calexcitin to functionally interact with protein partners and mediate its putative GTPase activity. An important observation in this respect is that of all of the metal-binding sites of calexcitin, EF-1 is the closest to the hydrophobic domain interface, which is known to be considerably affected by flexible protein motion (Erskine *et al.*, 2015). Earlier studies suggested that the binding of metal ions to the N-terminal domain reduces its molten-globule nature, thereby stabilizing the protein (Gombos *et al.*, 2003). During neuronal activation, the binding of Ca^{2+} to EF-1 as the Ca^{2+} concentration increases might cause an ordering of the hydrophobic residues which form the domain interface. Indeed, it is the domain interface which plays a key role in the interactions of EF-hand proteins with partner molecules in signalling cascades. It is important to bear in mind that both Ca^{2+} and Mg^{2+} are likely to bind to the protein, even though the overall affinity for Ca^{2+} is several orders of magnitude greater than that for Mg^{2+}. However, the intracellular concentration of Mg^{2+} is at least several orders of magnitude greater than the concentration of Ca^{2+}, and Mg^{2+} can thus compete very effectively with Ca^{2+} for the binding sites, especially when the intracellular Ca^{2+} concentration is low, for example in quiescent neurons. Gombos *et al.* (2003) argue that calcium signalling involves a constant competition between Ca^{2+} and Mg^{2+} for binding sites in signalling proteins and their experimental studies indicate that the N-terminal domain of calexcitin possesses two mixed Ca^{2+}/Mg^{2+}-binding sites, whereas the C-terminal domain probably has a more specific Ca^{2+}-binding site. Fully Ca^{2+}-bound calexcitin has been shown by solution NMR to undergo quite a drastic domain movement that is most likely to expose the hydrophobic inter-domain cleft and could then allow it to interact with partner proteins in signalling cascades (Erskine *et al.*, 2015). Indeed, these studies indicate that the fully Ca^{2+}-occupied form of calexcitin is predominantly in a domain-opened state in solution and thus the binding of Ca^{2+} to all three sites of calexcitin must trigger it to adopt a conformation which is capable of interacting with partner proteins. This is in agreement with studies performed on calmodulin, which have shown that the full conformational change upon calcium binding does not occur until all sites are occupied by Ca^{2+} following the displacement of Mg^{2+} from the protein (Malmendal *et al.*, 1999).

Thus, our results have corroborated previous findings on the Ca^{2+} affinities of the different metal-binding sites of calexcitin (Gombos *et al.*, 2003) and have provided some perspective on the previous conclusions that the C-terminal binding site is the sensor site (Erskine *et al.*, 2015). Furthermore, our new evidence that the N-terminal site is the lowest-affinity Ca^{2+} site opens possible avenues for research into how the N-terminal domain of calexcitin plays a functionally relevant role in the signalling events of learning and memory.

Acknowledgements

We acknowledge Diamond Light Source (Didcot, UK) for synchrotron beam time and user-support (award MX12342).

References

Adams, P. D. *et al.* (2010). *Acta Cryst.* D**66**, 213–221.
Alkon, D. L. (1979). *Science*, **205**, 810–816.
Alkon, D. L. (1983). *Sci. Am.* **249**, 70–84.
Alkon, D. L., Ikeno, H., Dworkin, J., McPhie, D. L., Olds, J. L., Lederhendler, I., Matzel, L., Schreurs, B. G., Kuzirian, A., Collin, C. & Yamoah, E. (1990). *Proc. Natl Acad. Sci. USA*, **87**, 1611–1614.
Beaven, G. D. E., Erskine, P. T., Wright, J. N., Mohammed, F., Gill, R., Wood, S. P., Vernon, J., Giese, K. P. & Cooper, J. B. (2005). *Acta Cryst.* F**61**, 879–881.
Borley, K. A., Epstein, H. T. & Kuzirian, A. M. (2002). *Biol. Bull.* **203**, 197–198.
Cates, M. S., Berry, M. B., Ho, E. L., Li, Q., Potter, J. D. & Phillips, G. N. (1999). *Structure*, **7**, 1269–1278.
Chen, V. B., Arendall, W. B., Headd, J. J., Keedy, D. A., Immormino, R. M., Kapral, G. J., Murray, L. W., Richardson, J. S. & Richardson, D. C. (2010). *Acta Cryst.* D**66**, 12–21.
Child, F. M., Epstein, H. T., Kuzirian, A. M. & Alkon, D. L. (2003). *Biol. Bull.* **205**, 218–219.
Cox, J. A., Winge, D. R. & Stein, E. A. (1979). *Biochimie*, **61**, 601–605.
Davis, I. W., Leaver-Fay, A., Chen, V. B., Block, J. N., Kapral, G. J., Wang, X., Murray, L. W., Arendall, W. B., Snoeyink, J., Richardson, J. S. & Richardson, D. C. (2007). *Nucleic Acids Res.* **35**, W375–W383.
Emsley, P. & Cowtan, K. (2004). *Acta Cryst.* D**60**, 2126–2132.
Emsley, P., Lohkamp, B., Scott, W. G. & Cowtan, K. (2010). *Acta Cryst.* D**66**, 486–501.
Epstein, H. T., Child, F. M., Kuzirian, A. M. & Alkon, D. L. (2003). *Neurobiol. Learn. Mem.* **79**, 127–131.
Erskine, P. T., Beaven, G. D., Hagan, R., Findlow, I. S., Werner, J. M., Wood, S. P., Vernon, J., Giese, K. P., Fox, G. & Cooper, J. B. (2006). *J. Mol. Biol.* **357**, 1536–1547.
Erskine, P. T., Fokas, A., Muriithi, C., Rehman, H., Yates, L. A., Bowyer, A., Findlow, I. S., Hagan, R., Werner, J. M., Miles, A. J., Wallace, B. A., Wells, S. A., Wood, S. P. & Cooper, J. B. (2015). *Acta Cryst.* D**71**, 615–631.
Evans, P. (2006). *Acta Cryst.* D**62**, 72–82.
Eyman, M., Crispino, M., Kaplan, B. B. & Giuditta, A. (2003). *Neurosci. Lett.* **347**, 21–24.
Giese, K. P., Peters, M. & Vernon, J. (2001). *Physiol. Behav.* **73**, 803–810.
Gombos, Z., Durussel, I., Ikura, M., Rose, D. R., Cox, J. A. & Chakrabartty, A. (2003). *Biochemistry*, **42**, 5531–5539.
Gombos, Z., Jeromin, A., Mal, T. K., Chakrabartty, A. & Ikura, M. (2001). *J. Biol. Chem.* **276**, 22529–22536.
Gombos, Z., Yap, K. L., Ikura, M. & Chakrabartty, A. (2006). *Biochem. Biophys. Res. Commun.* **343**, 520–524.
Gorrec, F. (2009). *J. Appl. Cryst.* **42**, 1035–1042.
Jancarik, J. & Kim, S.-H. (1991). *J. Appl. Cryst.* **24**, 409–411.
Kantardjieff, K. A. & Rupp, B. (2003). *Protein Sci.* **12**, 1865–1871.
Karplus, P. A. & Diederichs, K. (2012). *Science*, **336**, 1030–1033.
Kawai, R., Horikoshi, T., Yasuoka, T. & Sakakibara, M. (2002). *Neurosci. Res.* **43**, 363–372.
Kuzirian, A. M., Child, F. M., Epstein, H. T., Motta, M. E., Oldenburg, C. E. & Alkon, D. L. (2003). *Biol. Bull.* **205**, 220–222.
Kuzirian, A. M., Epstein, H. T., Buck, D., Child, F. M., Nelson, T. & Alkon, D. L. (2001). *J. Neurocytol.* **30**, 993–1008.

Lederhendler, I. I., Etchbberrigaray, R., Yamoah, E. N., Matzel, L. D. & Alkon, D. L. (1990). *Brain Res.* **534**, 195–200.
Leslie, A. G. W. & Powell, H. R. (2007). *Evolving Methods for Macromolecular Crystallography*, edited by R. J. Read & J. L. Sussman, pp. 41–51. Dordrecht: Springer.
Malmendal, A., Linse, S., Evenäs, J., Forsén, S. & Drakenberg, T. (1999). *Biochemistry*, **38**, 11844–11850.
McCoy, A. J., Grosse-Kunstleve, R. W., Adams, P. D., Winn, M. D., Storoni, L. C. & Read, R. J. (2007). *J. Appl. Cryst.* **40**, 658–674.
Moshiach, S., Nelson, T. J., Sanchez-Andres, J. V., Sakakibara, M. & Alkon, D. L. (1993). *Brain Res.* **605**, 298–304.
Murshudov, G. N., Skubák, P., Lebedev, A. A., Pannu, N. S., Steiner, R. A., Nicholls, R. A., Winn, M. D., Long, F. & Vagin, A. A. (2011). *Acta Cryst.* D**67**, 355–367.
Murshudov, G. N., Vagin, A. A. & Dodson, E. J. (1997). *Acta Cryst.* D**53**, 240–255.
Neary, J. T., Crow, T. & Alkon, D. L. (1981). *Nature (London)*, **293**, 658–660.
Nelson, T. J. & Alkon, D. L. (1988). *Proc. Natl Acad. Sci. USA*, **85**, 7800–7804.
Nelson, T. J. & Alkon, D. L. (1990). *Proc. Natl Acad. Sci. USA*, **87**, 269–273.
Nelson, T. J. & Alkon, D. L. (1995). *J. Neurochem.* **65**, 2350–2357.
Nelson, T. J. & Alkon, D. L. (1997). *Bioessays*, **19**, 1045–1053.
Nelson, T. J., Cavallaro, S., Yi, C.-L., McPhie, D., Schreurs, B. G., Gusev, P. A., Favit, A., Zohar, O., Kim, J., Beushausen, S., Ascoli, G., Olds, J., Neve, R. & Alkon, D. L. (1996). *Proc. Natl Acad. Sci. USA*, **93**, 13808–13813.
Nelson, T. J., Collin, C. & Alkon, D. L. (1990). *Science*, **247**, 1479–1483.
Nelson, T. J., Zhao, W.-Q., Yuan, S., Favit, A., Pozzo-Miller, L. & Alkon, D. L. (1999). *Biochem. J.* **341**, 423–433.
Newman, J., Egan, D., Walter, T. S., Meged, R., Berry, I., Ben Jelloul, M., Sussman, J. L., Stuart, D. I. & Perrakis, A. (2005). *Acta Cryst.* D**61**, 1426–1431.
Ohki, S., Ikura, M. & Zhang, M. (1997). *Biochemistry*, **36**, 4309–4316.
Silva, A. C. R. da, Kendrick-Jones, J. & Reinach, F. C. (1995). *J. Biol. Chem.* **270**, 6773–6778.
Sun, M.-K., Nelson, T. J., Xu, H. & Alkon, D. L. (1999). *Proc. Natl Acad. Sci. USA*, **96**, 7023–7028.
Winn, M. D. *et al.* (2011). *Acta Cryst.* D**67**, 235–242.
Wooh, J. W., Kidd, R. D., Martin, J. L. & Kobe, B. (2003). *Acta Cryst.* D**59**, 769–772.
Zheng, H., Chordia, M. D., Cooper, D. R., Chruszcz, M., Müller, P., Sheldrick, G. M. & Minor, W. (2014). *Nature Protoc.* **9**, 156–170.